

ORIGINAL ARTICLE

A Hierarchical Modelling Framework for Correcting Delayed Reporting in Spatio-Temporal Disease Surveillance Data

Oliver Stoner¹ | Theo Economou¹

¹Department of Mathematics, University of Exeter, UK

Correspondence
Laver Building, Exeter, EX4 4QE, UK.
Email: O.R.Stoner@exeter.ac.uk

Funding information
This work was funded by the Institute for Data Science and Artificial Intelligence, University of Exeter, UK.

Delayed reporting is a well established problem in the surveillance of infectious diseases such as dengue fever and influenza. For effective monitoring and intervention, it is crucial to be able to detect outbreaks well before they have been fully observed, based on any partial reports which may be available at the time. Here we propose a substantial spatio-temporal extension to an existing hierarchical modelling framework, to allow for structured and unstructured spatio-temporal variability in the incidence of disease cases and in the reporting delay mechanism itself. We apply a specific instance of this framework to severe acute respiratory infection (SARI) data from the state of Paraná, Brazil. We illustrate how between-region similarity in temporal and seasonal trends can be accounted for, and demonstrate the importance of flexibly allowing for dependence between regions.

KEYWORDS
Bayesian, censoring, Generalized Dirichlet, notification delay, under-reporting.

Abbreviations: SARI, severe acute respiratory infection; GDM, Generalized-Dirichlet-Multinomial.

1 | INTRODUCTION

Delayed reporting or ‘notification delay’ is where available count data are, for a time, an under-representation of the truth, owing to flaws or ‘lags’ in the data collection mechanism. In disease surveillance, delays such as those which occur during the transfer of information from local clinics to national surveillance centres mean that complete and informative counts of new cases are not immediately available. Often these delays are substantial, so that it can take several weeks or even months for the available data to reach a total reported count.

As an illustrative example, Figure 1 shows reported severe acute respiratory infection (SARI) cases across the whole state of Paraná, Brazil, in the weeks leading up to and including week t , the 16th week of 2017. At the end of week t , we only have data for cases reported that same week (here referred to as ‘within the first delay’), while for cases that occurred in week $t - 1$ we have data corresponding to both those reported during week $t - 1$ (the first delay) and during week t (the second delay). The number of available ‘delayed’ counts therefore increases by one for each week we go back into the past.

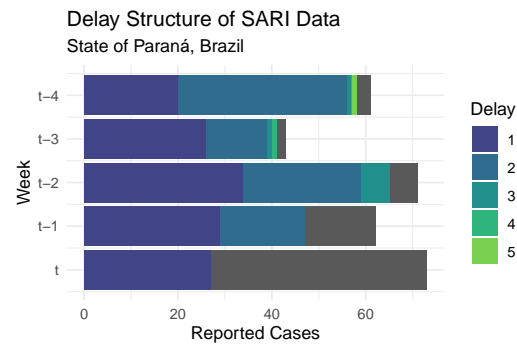


FIGURE 1 Bar plot of reported SARI cases in the weeks leading up to and including week t , the 16th week of 2017. The grey bars represent the total (as yet unobserved) number of reported cases, while the different coloured bars show the number of cases reported after each week of delay.

Variability in the delay mechanism (e.g. in the proportion of cases reported within one week) then makes it challenging to draw conclusions about the total counts in a timely manner. For example, more cases were reported within the first delay for week $t - 3$ than for week $t - 4$, but the total number of cases was much higher in week $t - 4$. At the end of week $t - 3$, this difference would only have been clear after waiting one more week until the number of cases for week $t - 3$ reported within the second delay became available. In disease surveillance, therefore, delayed reporting can make it difficult to confidently detect an outbreak within a time frame during which interventions are most effective.

From a statistical perspective, tackling delayed reporting is a prediction problem. Here, we would like to predict (now-cast) the present-day total count, as well as forecast future counts, based on any available partial counts and on any previous total counts which have now been fully observed. Appropriately utilising both sources of information motivates statistical modelling approaches which take into account both variability in the incidence of the total counts (e.g. of disease cases) and variability in the delay mechanism.

1.1 | Background

Stoner and Economou[1] present an overview of the well established biostatistical literature on modelling and correcting for delayed reporting, the vast majority of which deals with time series data. Notably, Höhle and an der Heiden[2] and Salmon et al.[3] both propose approaches based on a Multinomial mixture and apply them to Shiga toxin-producing *Escherichia coli* (STEC) and *Salmonella* data, respectively. In practice though, epidemiological applications (including

disease surveillance) often have a spatial dimension [4]. In such cases, we typically seek to take into account both structured and unstructured spatial variability in what we consider here to be the total counts (e.g. of disease cases). For example, the incidence rate of a particular disease might be more similar between nearby regions than between distant regions. Where data have both spatial and temporal dimensions, we may need to consider how spatial and temporal variability interact with one another. For example, a disease outbreak might be concentrated in a cluster of regions initially, but spread to more regions as time advances. However, the focus of this article is not only on how to account for spatio-temporal variability in the incidence of the total counts, but also on how to account for spatio-temporal variability in the model for the delay mechanism. For example, data from some regions may be available more quickly than data from others, and structured temporal variability in the delay mechanism may vary with space, e.g. due to changes over time in surveillance resourcing within individual regions.

The literature to date focusses solely on temporal variation, one exception being Bastos et al.[5] who deal with spatio-temporal data. There, the partial counts arriving after each delay interval are assumed Negative-Binomial in a Bayesian hierarchical framework. This approach, which was applied to spatio-temporal SARI data from Brazil, is quite flexible as it can potentially incorporate a wide variety of temporal, spatial and spatio-temporal structures. However, the total counts are not explicitly modelled, while the partial counts are assumed independent given covariates and random effects. As such, the distribution of the total counts may not be captured well, while excessive predictive uncertainty when now-casting and forecasting may also result [1].

Recently, Stoner and Economou[1] proposed a flexible yet interpretable framework for time series of count data affected by delayed reporting, which simultaneously models both the total counts and the delay mechanism. In this article we propose an extension to this framework which can incorporate spatio-temporal variability in both the model for the total counts and in the model for the delay mechanism. This is presented in the subsequent section, alongside a general discussion of spatial, temporal, and spatio-temporal structures which may be included in the model. In Section 3 we then apply a specific model within this framework to severe acute respiratory infection (SARI) data from Brazil, to illustrate how between-region similarity in temporal and seasonal trends can be accounted for. Finally, in Section 4 we present a critical discussion of our approach and highlight possible avenues for future research.

2 | MODELLING FRAMEWORK

We begin by introducing some notation. Let y_t be the total count occurring at time t and let $z_{t,d}$ be the part of y_t observed after $d = 1, \dots, D$ delays, so that $\sum_{d=1}^D z_{t,d} = y_t$. Stoner and Economou[1] present a multivariate hierarchical framework for simultaneously modelling y_t and $z_{t,d}$. An extension of this framework to include a spatial dimension $s \in S$ (e.g. districts, regions, countries) is given by:

$$y_{t,s} \mid \lambda_{t,s}, \theta_s \sim \text{Negative-Binomial}(\lambda_{t,s}, \theta_s); \quad (1)$$

$$\log(\lambda_{t,s}) = f(t, s); \quad (2)$$

$$z_{t,s} \sim \text{GDM}(\nu_{t,s}, \phi_{t,s}, y_{t,s}). \quad (3)$$

Structured spatio-temporal variability in the incidence of the total counts $y_{t,s}$ can be accounted for through the general function $f(t, s)$, which may include an offset (e.g. population), covariates or random effects. Variability in the delay mechanism is then modelled by the Generalized-Dirichlet-Multinomial (GDM) distribution, a Multinomial mixture where the parameter representing the vector of probabilities has a Generalized-Dirichlet distribution [6]. The use of this distribution for modelling the partial counts, instead of the more conventional Multinomial model, affords a great

deal of extra flexibility in accounting for over-dispersion in the delay mechanism (therefore improving the reliability of now-casting predictions) and in capturing unusual covariance structures in the partial counts [1]. Here we choose to parametrize the GDM in terms of parameters $\nu_{t,s}$ and $\phi_{t,s}$, where $\nu_{t,s,d} \in (0, 1)$ and $\phi_{t,s,d} > 0$ are respectively the mean and dispersion parameters of the Beta-Binomial conditional model for each individual partial count:

$$z_{t,s,d} \mid z_{t,s,-d}, y_{t,s} \sim \text{Beta-Binomial}(\nu_{t,s,d}, \phi_{t,s,d}, n_{t,s,d} = y_{t,s} - \sum_{j < d} z_{t,s,j}). \quad (4)$$

Two options were presented for modelling the relative means $\nu_{t,s,d}$. In the first (named the Hazard variant) they are modelled directly with a logit link, so that $\log(\nu_{t,s,d}/(1 - \nu_{t,s,d})) = g(t, s, d)$, for some general function $g(t, s, d)$. In the second (the Survivor variant) a model is first constructed for $S_{t,s,d}$, the expected cumulative proportion reported after delay d :

$$\text{probit}(S_{t,s,d}) = g(t, s, d), \quad (5)$$

where the probit function is the inverse-CDF of the Gaussian distribution. From these the relative means $\nu_{t,s,d}$ can be easily derived by computing $\nu_{t,s,d} = (S_{t,s,d} - S_{t,s,d-1})/(1 - S_{t,s,d-1})$. Stoner and Economou[1] argue that it is more intuitive to consider models for the cumulative proportion of $y_{t,s}$ reported by delay d , than to consider models for the expected proportion of $y_{t,s}$ reported at delay d out of those not already reported by delay $d - 1$, and so advocate adoption of the Survivor variant over the Hazard variant. The operational characteristics and performance (relative to other approaches) of both options have been studied extensively in Stoner and Economou[1].

In the next subsection we discuss how general functions $f(t, s)$ and $g(t, s, d)$ may be appropriately specified in a spatio-temporal context, specifically for the Survivor variant of the GDM framework.

2.1 | Spatio-temporal variability

Where missing information in the data arises solely from temporal delay in the reporting mechanism, it is worth considering the reasons for which joint modelling of the data across regions is needed, as opposed to applying a time series model to each region separately. One possible situation is a disease surveillance system where the sum of cases over a number of regions is important, e.g. for planning resource allocation on a larger geographical scale. Even if the joint (i.e. spatio-temporal) and independent (time series) models perform equally well at capturing the variance of the total counts in each region, the risk of not capturing similarities across multiple regions (e.g. in their temporal trends) is that the variance of any sum $V(S') = \text{Var}[\sum_{s \in S'} y_{t,s}] = \sum_{i \in S'} \sum_{j \in S'} \text{Cov}[y_{t,i}, y_{t,j}]$ for some $S' \subseteq S$, may not be captured well. The joint model is able to explicitly quantify the covariance of $y_{t,s}$ across regions (at least at the mean level which may indeed be sufficient), so that $(V(S'))$ may be captured better. In the case where missing information arises from other sources, e.g. data loss or national holidays, jointly modelling the regions is essential so that regions with less data can potentially borrow information from the others.

The selection of appropriate ways of capturing spatio-temporal variability is well-established in the field of epidemiology [7]. In disease count data, space is often defined by areal units, e.g. regions, counties etc. That said, it is possible to imagine relevant data which occur as continuous points in space, for example if counts represent the number of cases reported at individual clinics or hospitals. In either case, a sensible starting point in defining the model for the mean incidence rate, $f(t, s)$, is to consider separable functions of the form:

$$f(t, s) = f_1(t) + f_2(s) + f_3(t, s). \quad (6)$$

Here $f_1(t)$ allows for any common temporal or seasonal variation across the regions; $f_2(s)$ (which may include offsets such as population) allows for any overall differences in the mean of $y_{t,s}$ between regions; and $f_3(t, s)$ allows for deviations from the marginal temporal and spatial effects.

For the purposes of this article we need not restrict ourselves to any specific models for capturing spatio-temporal variability, among the many that are available to us (see for instance Banerjee et al.[8]), particularly as this choice is often application dependent. Instead we will briefly give some illustrative examples here and then we will discuss in more detail an approach based on nested spline structures, in our application to SARI data in Section 3.

Appropriate choices for $f_1(t)$ include independent Gaussian random effects (IGRE), Gaussian Markov random fields (GMRFs) such as random walks and autoregressive terms, dynamic linear models [9], Gaussian processes (GPs), or smoothing splines [10]. Choices for $f_2(s)$ include IGRE, GMRFs [11] (as adopted by Bastos et al.[5]), GPs for point data or indeed regression splines. Finally, choices for $f(t, s)$ include IGRE, independent temporally structured effects for each s (e.g. zero-centered splines), tensor product splines [12] or random effects which combine spatio-temporal interactions. For example, Kronecker products of GMRF models offer separable formulations [13][14][8].

Formulating the model for the expected cumulative proportion through $g(t, s, d)$ is slightly more complex due to the extra dimension, but can be decomposed in a similar manner, noting that in practice d is discrete and bounded from above. Here we consider separable functions of the form:

$$g(t, s, d) = g_1(t) + g_2(s) + g_3(d) + g_4(t, s) + g_5(t, d) + g_6(s, d) + g_7(t, s, d). \quad (7)$$

This characterisation allows for spatio-temporal variability in the delay mechanism, e.g. by including tensor product smoothing terms of time and delay which vary with space [12] or indeed treat d as a categorical variable and introduce interactions with terms involving s and t .

Again, the particular form of spatio-temporal characterisation is not of primary concern here, as all the methods we refer to above are well-established. It is important however to appreciate the need to structures involving interactions between space, time and delay, and to consider whether these make sense within the context of the application and the data. For instance, the delay mechanism may not, in some applications, vary across space s where this is defined at a small spatial scale (e.g. individual clinics or hospitals), but it may well vary across s at a larger scale (e.g. counties/regions). In the application to SARI data in Section 3, we opt for choices of $f(\cdot)$ and $g(\cdot)$ that are flexible yet practically feasible and appropriate to the application.

2.2 | Under-reporting

Often the total reported count, $y_{t,s,d}$, is still a substantial under-representation of the true count, termed here $x_{t,s,d}$. In disease surveillance for instance, under-resourcing and/or hard-to-reach areas lead to some cases being missed. To take this into account, Stoner and Economou[1] present a comprehensive framework for simultaneously modelling under-reporting and delayed-reporting. Extended here to a spatial context, this is achieved by replacing (1) with:

$$x_{t,s} \mid \lambda_{t,s}, \theta_s \sim \text{Negative-Binomial}(\lambda_{t,s}, \theta_s); \quad (8)$$

$$y_{t,s} \mid x_{t,s}, \pi_{t,s} \sim \text{Binomial}(\pi_{t,s}, y_{t,s}); \quad (9)$$

$$\log\left(\frac{\pi_{t,s}}{1 - \pi_{t,s}}\right) = i(t, s), \quad (10)$$

for $y_{t,s} \leq x_{t,s}$ and where $i(t, s)$ is a general function which may include covariates or random effects. The likelihood for $y_{t,s}$ is non-identifiable between a high $\lambda_{t,s}$ and a low $\pi_{t,s}$, or vice-versa, so in the case where all available counts are assumed potentially under-reported (i.e. $x_{t,s}$ is always unobserved), identifiability can be achieved using prior information[15].

3 | SEVERE ACUTE RESPIRATORY INFECTION DATA

The World Health Organization defines a severe acute respiratory infection (SARI) as an acute respiratory infection where the patient suffers from both a fever measured above 38°C and coughing, where hospitalization is necessary and where the onset of the infection was within the last 10 days [16]. One reason for this classification is to standardise surveillance of influenza-like illnesses, so that seasonal patterns in respiratory virus circulation can be studied and to inform prevention policies [5]. As explained in Bastos et al.[5], lags in data assimilation (from hospitals to local authorities, then to state and national levels) introduce delays in the information on SARI available to public health decision-makers, potentially inhibiting response to influenza outbreaks.

3.1 | Data

Here we use the data from the Brazilian state of Paraná, which was severely affected by the 2009 H1N1 epidemic compared to other states [17] and continues to have one of the highest rates of SARI incidence [5]. Here we consider a much longer time period of 230 weeks (from the start of January 2013 to the end of May 2017), compared to 66 weeks in Bastos et al.[5], to enable us to draw meaningful conclusions about seasonal variation. The state is divided into 22 health regions and we consider the total count to be fully observed 6 months after occurrence ($D = 27$). The dimension of the total counts $y_{t,s}$ is therefore 230×22 and the dimension of the partial counts $z_{t,s,d}$ is $230 \times 22 \times 27$ (corresponding to over 100k observations). For this application, we imagine that the present-day week, t_0 , is week 224 (mid April 2017). We then seek to make predictions for $t_0 = 224$, for previous weeks where the total count is still partially unobserved ($t = \{t_0 - D + 2, \dots, t_0 - 1\} = \{199, \dots, 223\}$) and for the next 6 weeks ($t = \{t_0 + 1, \dots, t_0 + 6\} = \{225, \dots, 230\}$).

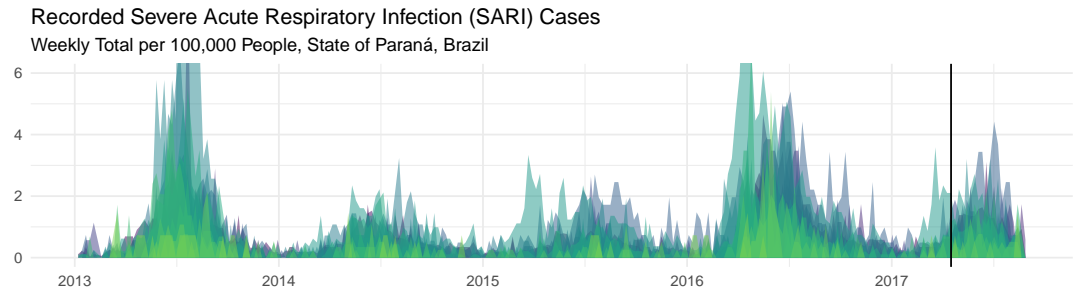


FIGURE 2 Area plot of total recorded SARI cases per 100,000 people, with a different colour for each of the 22 health regions. The vertical line shows the present week for this experiment $t_0 = 224$.

Figure 2 shows weekly total recorded SARI cases per 100,000 people by region. The plot shows a clear seasonal cycle across all regions, with outbreaks reaching their worst leading up to Brazil's with considerable year-to-year variability. There is also some evidence of regional variation in the overall rate – for example, the brightest green

region tends to have quite a low rate of cases per 100,000 people, compared to some other regions – as well as regional variation in the seasonal timing of outbreaks. At “present day” $t_0 = 224$, shown by the vertical line, we are in the early stages of the annual influenza outbreak, so forecasting predictions should ideally show an increasing trend in the number of SARI cases.

3.2 | Nested spline model

Stoner and Economou[1] present a model for a time series of dengue fever data in Rio de Janeiro, Brazil, where the incidence of the total recorded dengue counts is modelled by the combination of an intercept term, a temporal effect and a seasonal effect: $f(t) = \iota + \alpha_t + \eta_t$. The temporal (α_t) and seasonal (η_t) effects were defined using penalized cubic splines, and set up using the `jagam` function from the `mgcv` package for the R programming language [18]. This was shown to be a very flexible model in capturing smooth temporal and seasonal variation, so we also consider it here to describe the time series of SARI counts for any individual region. To capture spatio-temporal variability, we extend this to include spatially-varying intercept, temporal and seasonal effects:

$$f(t, s) = \iota_s + \delta_{t,s} + \xi_{t,s}; \quad (11)$$

with ι_s assigned a non-informative $\text{Normal}(0, 10^2)$ prior distribution and $\delta_{t,s}$ and $\xi_{t,s}$ being penalized cubic splines for each region. Each regional spline, say $\delta_{t,s}$, is defined by $\delta_{t,s} = \mathbf{X}_t \boldsymbol{\kappa}_s^{(\delta)}$. Here \mathbf{X}_t is a model matrix of the basis functions evaluated at each time point, and $\boldsymbol{\kappa}_s^{(\delta)}$ is a vector of coefficients. To penalize the splines for over-fitting, the coefficients are assigned a Multivariate-Normal prior with mean zero and precision matrix $\boldsymbol{\Omega}_s^{(\delta)} = \tau_s^{(\delta)} \mathbf{M}_s^{(\delta)}$. Matrix $\mathbf{M}_s^{(\delta)}$ is a known non-diagonal matrix, scaled by a smoothing (penalty) parameter $\tau_s^{(\delta)}$ [18], so that larger values of $\tau_s^{(\delta)}$ result in a smoother $\delta_{t,s}$ for each s .

However, Figure 2 suggests that a large portion of temporal and seasonal variation may be common across all regions. To take this into account, we can introduce temporal and seasonal effects α_t and η_t , and make their (basis function) coefficients the mean of the coefficients for the regional effects $\delta_{t,s}$ and $\xi_{t,s}$, i.e.

$$\alpha_t = \mathbf{X}_t \boldsymbol{\kappa}^{(\alpha)}; \quad (12)$$

$$\boldsymbol{\kappa}^{(\alpha)} \sim \text{Multivariate-Normal}(\mathbf{0}, \boldsymbol{\Omega}^{(\alpha)} = \tau^{(\alpha)} \mathbf{M}_s^{(\alpha)}); \quad (13)$$

$$\boldsymbol{\kappa}_s^{(\delta)} \sim \text{Multivariate-Normal}(\boldsymbol{\kappa}^{(\alpha)}, \boldsymbol{\Omega}_s^{(\delta)}). \quad (14)$$

Functions α_t and η_t capture the common temporal and seasonal variation across all regions respectively, while $\delta_{t,s}$ and $\xi_{t,s}$ capture regional deviations from these overall trends. Parameters $\tau^{(\alpha)}$ and $\tau^{(\eta)}$ therefore penalize the overall effects for smoothness, while $\tau_s^{(\delta)}$ and $\tau_s^{(\xi)}$ penalize the smoothness of the regional deviations from the overall effects. The main advantage of this structure – which can be efficiently implemented using Markov Chain Monte Carlo (MCMC) owing to the conjugate relationship between the Multivariate-Normal priors for the overall effects and the regional deviations – is that α_t and η_t can capture temporal and seasonal covariation between regions, an important feature for some applications as discussed in Section 2.1. This approach to pooling information, while allowing for individual variability, was shown to be very effective in modelling global polluting cooking-fuel usage, so that countries with little data could borrow information from regional trends [19].

We adopt the same approach when extending the relatively simple model used in Stoner and Economou[1] for the

expected cumulative proportion reported at each delay, $g(t, d) = \psi_d + \beta_t$, to include spatial variability:

$$g(t, s, d) = \psi_{s,d} + \gamma_{t,s}. \quad (15)$$

Here fixed delay effects $\psi_{s,d}$ are independent across regions and assigned non-informative first order random walk prior distributions, i.e. $\psi_{s,d} \sim \text{Normal}(\psi_{s,d-1}, 10^2)$, but truncated such that $\psi_{s,d} > \psi_{s,d-1}$ (to respect the fact that the cumulative proportion should increase with d). As in the model for $f(t, s)$, temporal effects $\gamma_{t,s}$ are penalized cubic splines centred on an overall temporal trend β_t (as in (12)-(14)).

3.3 | Prior distributions and implementation

Prior distributions for other parameters were chosen to constrain the parameter space to reasonable values (in relation to the data) but without being overly informative: For the Negative-Binomial dispersion parameters θ_s we specified independent Gamma(2,0.02) prior distributions, where the 95% credible interval [12.1, 279] covers high levels of over-dispersion (e.g. $\theta_s = 20$), while more extreme levels (e.g. $\theta_s = 10$) are less likely a-priori. We also specified Gamma(2,0.02) priors for the Beta-Binomial dispersion parameters $\phi_{s,d}$, following the same reasoning. Finally, it can be more interpretable to parametrize the spline precision penalties (e.g. $\tau_s^{(\delta)}$) as standard-deviation penalties (i.e. $\sigma_s^{(\delta)} = 1/\sqrt{\tau_s^{(\delta)}}$), so that smaller values for $\sigma_s^{(\delta)}$ correspond to a stricter penalty. For these we specified positive Half-Normal(0,1) prior distributions, meaning smoother functions are more likely a-priori.

As discussed in Stoner and Economou[1], instead of explicitly modelling all available partial counts $z_{t,s,d}$, we can reduce computational complexity by choosing to only explicitly model counts for $d \leq D' \leq D$. This is achieved by only including the conditional Beta-Binomial models for $z_{t,s,d}$ up to D' , so that the remainder $r_{t,s} = y_{t,s} - \sum_{d=D'+1}^D z_{t,s,d}$ is modelled implicitly. The trade-off associated with this choice is that predictive precision for $y_{t,s,d}$ is reduced, but generally only for past weeks $t \leq t_0 - D'$. Hence selecting a small D' may be considered a pragmatic choice where optimally precise predictions are not needed far into the past. In this experiment we opt for $D' = 2$, which we consider sensible in a situation where optimally precise predictions are not needed for two weeks or more into the past.

All code was written and executed in the R programming language [20]. The model was implemented using the `nimble` package [21], which offers facilities for highly flexible implementation of Bayesian models using MCMC. Eight MCMC chains were run from different randomly generated initial values and with different random number generator seeds. We ran the chains for 2000k iterations, discarding 1000k as burn-in and then thinning by 1000. Convergence of the MCMC chains was assessed by computing the potential scale reduction factor (PSRF) [22] for samples of each $\lambda_{t,s}$, of each θ_s and of each partially unobserved $y_{t,s}$ (i.e. the parameters associated with now-casting and forecasting). By convention, starting multiple chains from different initial values, with different random number generator seeds, and obtaining a PSRF close to or less than 1.05 for a given parameter is taken to indicate convergence. Here, all of the PSRFs for the θ_s were less than 1.05, as well as virtually all of the $\lambda_{t,s}$ (>99%) and the overwhelming majority of the $y_{t,s}$ (>93%, with >99% less than 1.2).

3.4 | Results

Figure 3 shows median predicted temporal ($\delta_{t,s}$, left) and seasonal ($\xi_{t,s}$, centre) effects on SARI incidence, as well as the temporal effect on the cumulative proportion reported ($\gamma_{t,s}$, right). A different colour is used for each region and the dashed black lines show the median predicted overall effects, α_t , η_t and β_t , respectively. The estimated effects on SARI incidence follow the overall trends quite closely, with only a few deviating substantially. For example, there are

noticeable increases in the temporal effect on SARI incidence for almost all regions around mid 2013 and around mid 2016, corresponding to the two largest outbreaks seen in Figure 2. Similarly, all the seasonal effects reflect the increase in SARI incidence leading up to Brazil's winter seen in Figure 2. The effects on the cumulative proportion reported are substantially more variable, suggesting that the delay mechanism may be driven more by local factors compared to SARI incidence.

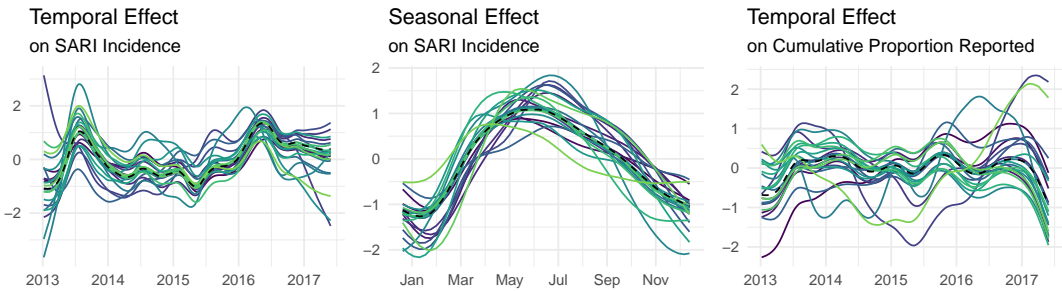


FIGURE 3 Median predicted temporal and seasonal effects on SARI incidence (left and centre) and median predicted temporal effect on the cumulative proportion reported (right).

Summarising, the 22 health regions of Paraná have a lot in common, in terms of temporal and seasonal variation in SARI incidence. It is worth examining, however, whether anything tangible was gained from modelling the regions simultaneously as opposed to using 22 independent time series models. In Section 2.1, we argued that modelling the regions independently could impede the model's ability to capture the variance of the total number of reported cases across all regions. To assess this, we applied 22 independent models where $f(t) = \iota + \delta_t + \xi_t$ and $g(t, d) = \psi_d + \gamma_t$ for each region. We then used posterior predictive checking [23] to see which approach captures the variance of the total better.

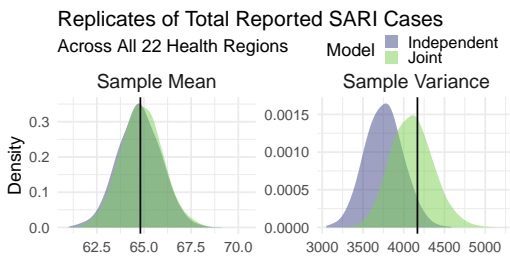


FIGURE 4 Posterior replicates of the sample mean (left) and sample variance (right) of fully observed ($t \leq t_0 - D + 1$) total reported number of SARI cases across all 22 health regions. Vertical lines show the corresponding observed statistics.

Figure 4 shows posterior replicates of the sample mean and sample variance of fully observed ($t \leq t_0 - D + 1$) total reported number of SARI cases across all 22 health regions (i.e. the total for the whole state). Both models perform equally well at capturing the mean number of cases, but notably the joint model is overwhelmingly better at capturing the sample variance compared to the independent models – the observed sample variance is firmly in the centre of the replicate distribution from the joint model. This suggests that the joint model is more appropriate in applications where predictions are also important at a larger geographical scale.

Finally, we can examine the model's ability to now-cast and forecast. Figure 5 shows predicted total reported SARI cases in the three most populous regions of Paraná: Curitiba (left), Londrina (centre) and Maringá (right). Among these

three regions, the forecasting predictions when fitted at present week $t_0 = 224$ appear most precise for Curitiba and Londrina, while somewhat over-predicting the number of cases in Maringá. This over-prediction is common across many of the regions, likely owing to the reduced magnitude of the outbreak compared to the previous year, which the model may detect when fitted further into the outbreak. That said, virtually all of the observations are within the 95% prediction intervals, with precise now-casting predictions for the present week (shown by the vertical line), which are all within the 50% prediction intervals.

For this experiment, the overall 95% prediction interval coverage was 0.99 for predictions of the total reported count corresponding to previous weeks ($t < t_0$), 1 when forecasting ($t > t_0$) and 1 when now-casting ($t = t_0$).

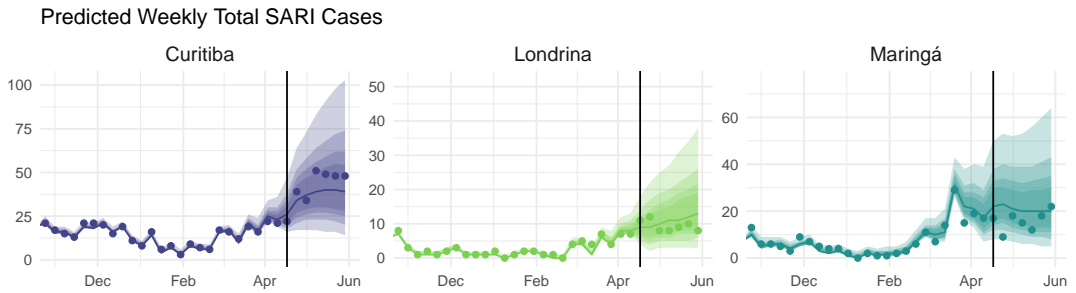


FIGURE 5 Predicted (median, 50%, 65%, 80%, and 95% prediction intervals) total reported SARI cases for the three most populous health regions. The vertical lines show the present week $t_0 = 224$.

4 | DISCUSSION

To bring the well-established literature on modelling delayed reporting in line with modern disease surveillance applications, we have presented a spatio-temporal extension to demonstrably the most flexible and best-performing framework for modelling delayed reporting in count data available. The framework allows for a wide variety of spatial, temporal, and spatio-temporal structures to be included in both the model for the total reported counts after any delays have passed, and in the model for the delay mechanism itself. To illustrate how the framework can be used to take into account similarity in temporal and seasonal structures between regions, we have applied our framework to severe acute respiratory infection (SARI) data from the Brazilian state of Paraná.

Though the spatio-temporal model for SARI data presented here is quite intuitive and demonstrably better than independent time series models when aggregating predictions to a super-regional level, it may be overly simplistic: Firstly, while our nested spline approach enabled the model to capture the distribution of the total counts across all regions well, both the model for SARI incidence and the delay model lack any explicit spatial structure (i.e. the model assumes equivalent similarity between all regions). In applications where some regions have a lot of missing data, models with explicit spatial structure may allow for more precise predictions in those regions. A lack of data may also warrant including spatial structure in the dispersion parameters, which is possible by modelling them as log-linear [1].

Secondly, a lack of a delay-time interaction term in the model for the expected cumulative proportion reported may be responsible for the excessively high 95% prediction interval coverage values (corresponding to under-confident predictions) quoted in Section 3.4. More serious applications might therefore benefit from considering more complicated mean delay models, which are of course possible within the framework proposed here. Depending on the frequency

with which predictions need to be updated, any further extension of the model may be potentially hindered by the fact that our model is quite computationally expensive, taking around a day to run on a high-end desktop computer in 2019. This is in part due to the size of the data – as an illustrative example, considering 230 weeks and 22 regions results in 5060 total counts to compute the likelihood for and/or sample at each iteration. Substantial gains in efficiency might therefore be obtained by parallelising the within-chain MCMC computations (see Goudie et al.[24]) or deriving an approximate Bayesian method for implementing the Generalized-Dirichlet-Multinomial.

Using the framework presented here it is possible to comprehensively address the problem of delayed reporting in spatio-temporal applications. This ignores, however, the possible problem of substantial under-reporting in the final reported counts, as described in Section 2.2. Therefore any predictions from models discussed here, e.g. of disease cases, may lead to an undersized response to the true magnitude of an outbreak. Although we have explained how under-reporting can be taken into account within the modelling framework we propose, this approach has so far only been applied in a purely hypothetical scenario (see [25]). Future research should therefore be directed at applications where effective disease surveillance is inhibited by both delayed reporting and under-reporting.

CONFLICT OF INTEREST

The authors declare no potential conflict of interests.

SUPPORTING MATERIAL

The SARI data and R code necessary to reproduce all results in this article are included as supporting material.

REFERENCES

- [1] Stoner O, Economou T. Multivariate hierarchical frameworks for modelling delayed reporting in count data. *Biometrics* 2019;<https://onlinelibrary.wiley.com/doi/abs/10.1111/biom.13188>.
- [2] Höhle M, an der Heiden M. Bayesian nowcasting during the STEC O104:H4 outbreak in Germany, 2011. *Biometrics* 2014 6;70(4):993–1002. <https://doi.org/10.1111/biom.12194>.
- [3] Salmon M, Schumacher D, Stark K, Höhle M. Bayesian outbreak detection in the presence of reporting delays. *Biometrical Journal* 2015;57(6):1051–1067. <https://onlinelibrary.wiley.com/doi/abs/10.1002/bimj.201400159>.
- [4] Cabrera M, Taylor G. Modelling spatio-temporal data of dengue fever using generalized additive mixed models. *Spatial and Spatio-temporal Epidemiology* 2019;28:1 – 13. <http://www.sciencedirect.com/science/article/pii/S1877584517301363>.
- [5] Bastos LS, Economou T, Gomes MFC, Villela DAM, Coelho FC, Cruz OG, et al. A modelling approach for correcting reporting delays in disease surveillance data. *Statistics in Medicine* 2019;38(22):4363–4377. <https://onlinelibrary.wiley.com/doi/abs/10.1002/sim.8303>.
- [6] Wong TT. Generalized Dirichlet distribution in Bayesian analysis. *Applied Mathematics and Computation* 1998;97(2):165 – 181. <http://www.sciencedirect.com/science/article/pii/S0096300397101400>.
- [7] Shaddick G, Zidek J. *Spatio-Temporal Methods in Environmental Epidemiology*. CRC Texts in Statistical Science, United Kingdom: Chapman & Hall; 2015.
- [8] Banerjee S, Carlin BP, Gelfand AE. *Hierarchical Modeling and Analysis for Spatial Data*. CRC Press; 2014.

- [9] Petris G, Petrone S, Campagnoli P. *Dynamic Linear Models with R*. Use R!, Springer New York; 2009. <https://books.google.co.uk/books?id=VCt3zVq8T08C>.
- [10] Wood SN. *Generalized Additive Models: An Introduction with R*, Second Edition (Chapman and Hall/CRC Texts in Statistical Science). Second ed. London: Chapman and Hall/CRC; 2017.
- [11] Besag J, York J, Mollié A. Bayesian image restoration, with two applications in spatial statistics. *Annals of the Institute of Statistical Mathematics* 1991 Mar;43(1):1–20. <https://doi.org/10.1007/BF00116466>.
- [12] Wood SN. Low-Rank Scale-Invariant Tensor Product Smooths for Generalized Additive Mixed Models. *Biometrics* 2006;62(4):1025–1036. <https://onlinelibrary.wiley.com/doi/abs/10.1111/j.1541-0420.2006.00574.x>.
- [13] Lindgren F, Rue H. Bayesian Spatial Modelling with R-INLA. *Journal of Statistical Software, Articles* 2015;63(19):1–25. <https://www.jstatsoft.org/v063/i19>.
- [14] Cameletti M, Lindgren F, Simpson D, Rue H. Spatio-temporal modeling of particulate matter concentration through the SPDE approach. *AStA Advances in Statistical Analysis* 2013 Apr;97(2):109–131. <https://doi.org/10.1007/s10182-012-0196-3>.
- [15] Stoner O, Economou T, Drummond Marques da Silva G. A Hierarchical Framework for Correcting Under-Reporting in Count Data. *Journal of the American Statistical Association* 2019a;.
- [16] World Health Organization, WHO surveillance case definitions for ILI and SARI; 2014. Accessed 2019-09-25. https://www.who.int/influenza/surveillance_monitoring/ili_sari_surveillance_case_definition/en/.
- [17] Codeço CT, Cordeiro JdS, Lima AWdS, Colpo RA, Cruz OG, Coelho FC, et al. The epidemic wave of influenza A (H1N1) in Brazil, 2009. *Cadernos de saúde pública* 2012;28(7):1325–1336.
- [18] Wood S. Just Another Gibbs Additive Modeler: Interfacing JAGS and mgcv. *Journal of Statistical Software, Articles* 2016;75(7):1–15. <https://www.jstatsoft.org/v075/i07>.
- [19] Stoner O, Shaddick G, Economou T, Gumy S, Lewis J, Lucio I, et al., Global Household Energy Model: A Multivariate Hierarchical Approach to Estimating Trends in the Use of Polluting and Clean Fuels for Cooking; 2019b.
- [20] R Core Team. *R: A Language and Environment for Statistical Computing*. R Foundation for Statistical Computing, Vienna, Austria; 2019, <https://www.R-project.org/>.
- [21] de Valpine P, Turek D, Paciorek CJ, Anderson-Bergman C, Lang DT, Bodik R. Programming With Models: Writing Statistical Algorithms for General Model Structures With NIMBLE. *Journal of Computational and Graphical Statistics* 2017;26(2):403–413. <https://doi.org/10.1080/10618600.2016.1172487>.
- [22] Brooks SP, Gelman A. General Methods for Monitoring Convergence of Iterative Simulations. *Journal of Computational and Graphical Statistics* 1998;7(4):434–455. <https://www.tandfonline.com/doi/abs/10.1080/10618600.1998.10474787>.
- [23] Gelman A, Carlin J, Stern H, Dunson D, Vehtari A, Rubin D. *Bayesian Data Analysis*, Third Edition (Chapman and Hall/CRC Texts in Statistical Science). Third ed. London: Chapman and Hall/CRC; 2014.
- [24] Goudie RJB, Turner RM, De Angelis D, Thomas A. MultiBUGS: A parallel implementation of the BUGS modelling framework for faster Bayesian inference. *arXiv e-prints* 2017 Apr;p. arXiv:1704.03216.
- [25] Stoner O. *Bayesian Hierarchical Modelling Frameworks for Flawed Data in Environment and Health*. PhD thesis, University of Exeter; 2019.